Acute and Chronic Changes in the Microcirculation of the Liver in Inbred Strains of Mice Following Infection with Mouse Hepatitis Virus Type 3

PEGGY J. MACPHEE, VINCENT J. DINDZANS, LAI-SUM FUNG AND GARY A. LEVY

Liver Disease Unit, Sunnybrook Medical Center, University of Toronto, Toronto, Ontario, Canada M4N 3M5

The acute and chronic effects of mouse hepatitis virus type 3 on the microcirculation of the liver in both semisusceptible C3HeB/FeJ and fully resistant A/J mice were studied. In the C3HeB/FeJ mice, abnormalities of microcirculatory flow were noted as early as 12 hr after infection and by 24 hr, localized avascular foci appeared. Disturbances were characterized by granular blood flow, sinusoidal microthrombi, distortion of sinusoids by edematous hepatocytes and necrotic lesions. Following the acute infection, Day 10, two patterns of chronic disease were observed. Eighty percent of the mice developed chronic granulomatous hepatitis whereas in the remaining 20% a more severe chronic aggressive hepatitis was observed which was characterized by ongoing hepatocellular necrosis and a marked mononuclear cell infiltrate. In both cases, in vivo microcirculatory abnormalities were found predominantly around visible lesions. Onset of the microcirculatory abnormalities was found to be concomitant with a rise in monocyte related procoagulant activity. Procoagulant activity rose acutely and remained elevated throughout the chronic phase but was higher in animals with severe disease. In contrast to the above, normal blood flow and histology were seen in the resistant A/J mice at all times following infection, and procoagulant activity remained at basal levels despite active viral replication as demonstrated by immunofluorescence studies and recovery of infectious virus. These observations suggest a role for monocyte procoagulant activity in the development of microcirculatory abnormalities following mouse hepatitis virus type 3 infection which may be important in the pathogenesis of the disease.

The liver is dependent on a specialized and abundant blood supply for its intense and diverse metabolic activity (1). The parenchyma of the liver is comprised of a heterogeneous population of hepatocytes organized by the final radicles of the microcirculation into simple liver acini, the smallest structural and functional units of the

liver (2). The sinusoids of the simple liver acini along with the nutrient portal triad and draining terminal hepatic venule comprise the basic microvascular unit of the liver. Oxygen levels, blood composition, flow and pressure in the microcirculation contribute to a local environment which is in dynamic balance with the functionally heterogeneous hepatocytes across the simple liver acini; this is reflected by significant gradients in oxygen tension, redox state and cytoplasmic enzyme activities across zones 1 to 3 (3, 4). Selective zonal injury to the hepatic parenchymal plate by toxic agents in turn results in localized zonal abnormalities of the microcirculation (5, 6).

Infection with mouse hepatitis virus type 3 (MHV-3), a member of the single-stranded, positive polarity, RNA-containing coronaviruses, causes a strain-dependent spectrum of liver disease in inbred mice (7). Mice of fully susceptible strains (Balb/cJ, C57Bl/6J and DBA) die of fulminant hepatitis; mice of semisusceptible strains (C3H/St, C3HeB/FeJ) develop acute hepatitis which

ultimately results in chronic liver disease while resistant adult mice (A/J) develop no liver disease. Previous experiments showed that viral replication occurs to comparable levels in resistant as well as susceptible mice, hence it is apparent that viral replication alone contributes only in part to the pathogenesis of viral hepatitis (8). Experimental evidence has suggested that host-immune defects may have a major role in determining strain-dependent susceptibility to MHV-3 infection (8).

We have previously shown that strain-dependent susceptibility to MHV-3 correlates directly with the spontaneous T lymphocyte controlled expression of a procoagulant monokine which exhibits prothrombin cleaving activity [procoagulant activity (PCA)] (9). A biological role for this activity in the pathogenesis of liver disease has been suggested by in vivo microscopic observations during acute MHV-3 infection in the fully susceptible Balb/cJ strain (8). In this system, abnormalities of the microcirculation consisting of granular blood flow and sinusoidal microthrombi preceded in vivo viral replication by 24 hr. Subsequently, focal thrombotic and/or ischemic lesions formed and finally resulted in confluent liver necrosis.

The present study was designed to examine the hepatic microcirculation during both the acute and chronic phases of MHV-3 infection in mice of the semisusceptible C3HeB/FeJ strain (7, 10). The in vivo hepatic microcirculation was studied and compared with both the spontaneous expression of monocyte/macrophage PCA and histological parameters of liver disease.

MATERIALS AND METHODS

VIRUS

The origin and growth of MHV-3 has been previously described (9). MHV-3, obtained from the American Type Culture Collection, Rockville, Md. (ATTCC VR 262), was plaque-purified on monolayers of DBT cells. Stock virus was grown to a titer of 1.2×10^7 plaque-forming units per ml in 17 CL1 cells. The virus was harvested by one cycle of freeze thawing and clarified by centrifugation at $4,500 \times g$ for 1 hr at 4°C. Virus was assayed on monolayers of L2 cells in a standard plaque assay (9).

Viral purification was accomplished by centrifugation through polyethylene glycol and sequential potassium tartrate gradients (11). Purified virus at a titer of 1.2×10^9 plaque-forming units per ml was finally resuspended in normal saline.

MICE

A/J and C3HeB/FeJ mice, 6 to 8 weeks of age, were obtained from Jackson Laboratories, Bar Harbor, Maine. The presence of serum antibody to mouse hepatitis virus was ruled out by a standard radioimmunoassay as described previously (11). Mice were i.p. injected with 10^3 plaque-forming units of stock MHV-3 in 0.1 ml. of Dulbecco's modified Eagle's medium (DMEM). They were followed for up to 4 months and sacrificed at various time intervals. Blood was obtained by axillary bleeding; samples of liver tissue were processed for immunofluorescence, viral titers and routine H and E histology.

IMMUNOFLUORESCENCE

A heterologous antibody to MHV-3 was produced in New Zealand White male rabbits by hyperimmunization with purified MHV-3 in complete Freund's adjuvant (8). The antiserum was found to be suitable for use at 1/40 dilution. Immunofluorescence was studied by an indirect method using a fluorescein-labeled goat antirabbit IgG as the probe. By radioimmunoprecipitation, the antibody demonstrated predominant specificity for the nucleocapsid protein with weak E1 and E2 envelope glycoprotein reactivity.

VIRAL TITERS

Liver tissue was homogenized in DMEM as a 10% homogenate (w/v) at 4°C. Viral titers were then determined on monolayers of L2 cells in a standard plaque assay (9).

ISOLATION OF PERIPHERAL BLOOD MONONUCLEAR CELLS (PBMs)

Heparinized blood from 10 mice for each time point was pooled and suspended in an equal volume of DMEM. Mononuclear cells were isolated over Ficoll-Hypaque gradients by centrifugation at 22°C at $2,200 \times g$ for 12 min. Cells at the interface were collected and found to be greater than 98% mononuclear cells by cytologic examination using Giemsa stain. Viability was greater than 99% by trypan blue exclusion. Cells were washed twice and resuspended in DMEM at a concentration of 2×10^6 mononuclear cells per ml.

ISOLATION OF SPLEEN CELLS

Spleens were removed aseptically from C3HeB/FeJ mice, and cells were suspended in DMEM. Mononuclear cells were isolated by centrifugation over Ficoll-Hypaque at 22°C for 12 min at $2,200 \times g$. Cells from the interface were greater than 98% mononuclear by cytologic examination. Cells were washed twice and resuspended in DMEM at a concentration of 2×10^6 mononuclear cells per ml.

PCA

Samples of viable cells or cells which were subjected to three cycles of freeze thawing and sonication were assayed for the capacity to shorten the spontaneous clotting time of normal citrated human plasma in a one-stage clotting assay (12). To 0.1 ml of cellular homogenate or viable cells at 4°C, 0.1 ml of citrated normal human platelet-poor plasma or factor-deficient plasma (Helena Laboratories, Beaumont, Tex.) was added, followed by 0.1 ml of 25 mM $CaCl_2$ to start the reaction. The time for the appearance of a fibrin gel was recorded. Clotting times were converted to units of PCA by comparison to a rabbit brain thromboplastin standard (Dade Division, American Hospital Supply, Miami, Fla.) where 36 mg dry weight per ml were assigned a value 100,000 mU PCA. The assay was utilized over the range of 1 to 100,000 mU or 10^2 to 10^8 cells, and it was linear over this range with normal plasma substrate. Media with or without 10% fetal calf serum and buffers were all without activity.

HEPATIC MICROCIRCULATION

Mice were injected i.p. with 1,000 PFU of stock MHV-3 in 0.1 ml DMEM and examined at various time intervals. Control mice were injected with 0.1 ml of DMEM. Anesthesia was obtained with Nembutal (6.4 mg per 100 gm body weight) by i.p. injection. The animals were immobilized on a heated surgical table with temperature control at 37°C. Mice were intubated (PE-10 intramedic tubing, Clay Adams, NY) by tracheostomy and ventilated with room air by a volume ventilator at 50 cycles per min and 2 ml per breath. Laparotomy by midline incision was performed, and the peritoneal cavity was irrigated with Ringer's lactate solution warmed to 37°C. Tubocurare (0.02 ml of 3 mg per ml solution) was injected intramuscularly as required. The liver margin was transilluminated with a quartz rod connected to a fiberoptic light source (Intralux 150H Volpi, Zurich, Switzerland). The microcirculation was observed through an E. Leitz microscope as previously described (8).

RESULTS

LIVER HISTOLOGY

No abnormalities in liver histology could be found in A/J mice for up to 21 days following infection (Figure 1A). In contrast, at 24 hr, the livers from C3HeB/FeJ mice had focal necrotic lesions consisting of acidophilic degenerating hepatocytes and nuclear debris with a sparse inflammatory infiltrate (Figure 2A). By 3 days postinfection, these early lesions became larger, more numerous and were associated with an infiltrate of pyknotic polymorphonuclear leukocytes (Figure 2C). At 5 days, confluent necrosis was evident in some sections (Figure 3A). By 7 to 10 days, the lesions were densely infiltrated with intact mononuclear cells, and the adjoining liver parenchyma underwent intense hepatocyte regeneration as evidenced by many mitotic figures (Figure 4A). Following the acute phase of the disease (Day 10), two patterns of chronic disease were observed. The first was characterized by the appearance of epithelioid cells with large pale nuclei and pale granular cytoplasm. These appeared within the foci of necrosis by 11 days postinfection, and by Day 15, most remaining lesions were organized into granulomas consisting of centralized epithelioid cells surrounded by mononuclear cells (Figure 4C). From Day 21 until 3 months, the liver histology was characterized by perivascular mononuclear cell infiltrates usually associated with the terminal portal venule and giant cell granulomas (Figure 5A). A second pattern
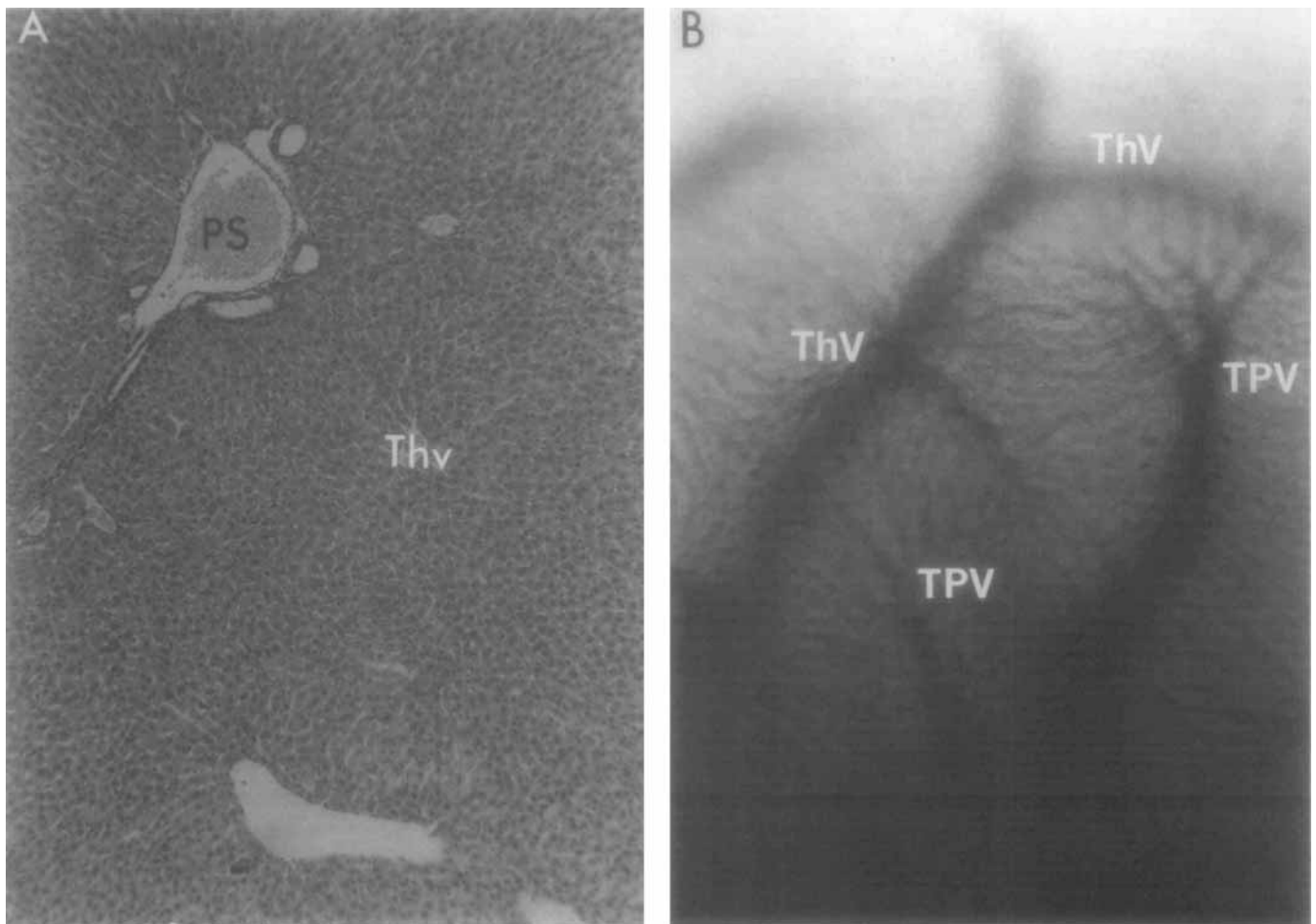

FIG. 1. Studies of A/J livers 3 days following MHV-3 infection. (A) A normal portal space (PS) and terminal hepatic venule (Thv) (H & E, × 550). (B) *In vivo* microscopy showing normal microcirculation at the liver margin with alternating terminal portal venules (TPV) and terminal hepatic venules (ThV) (× 550).
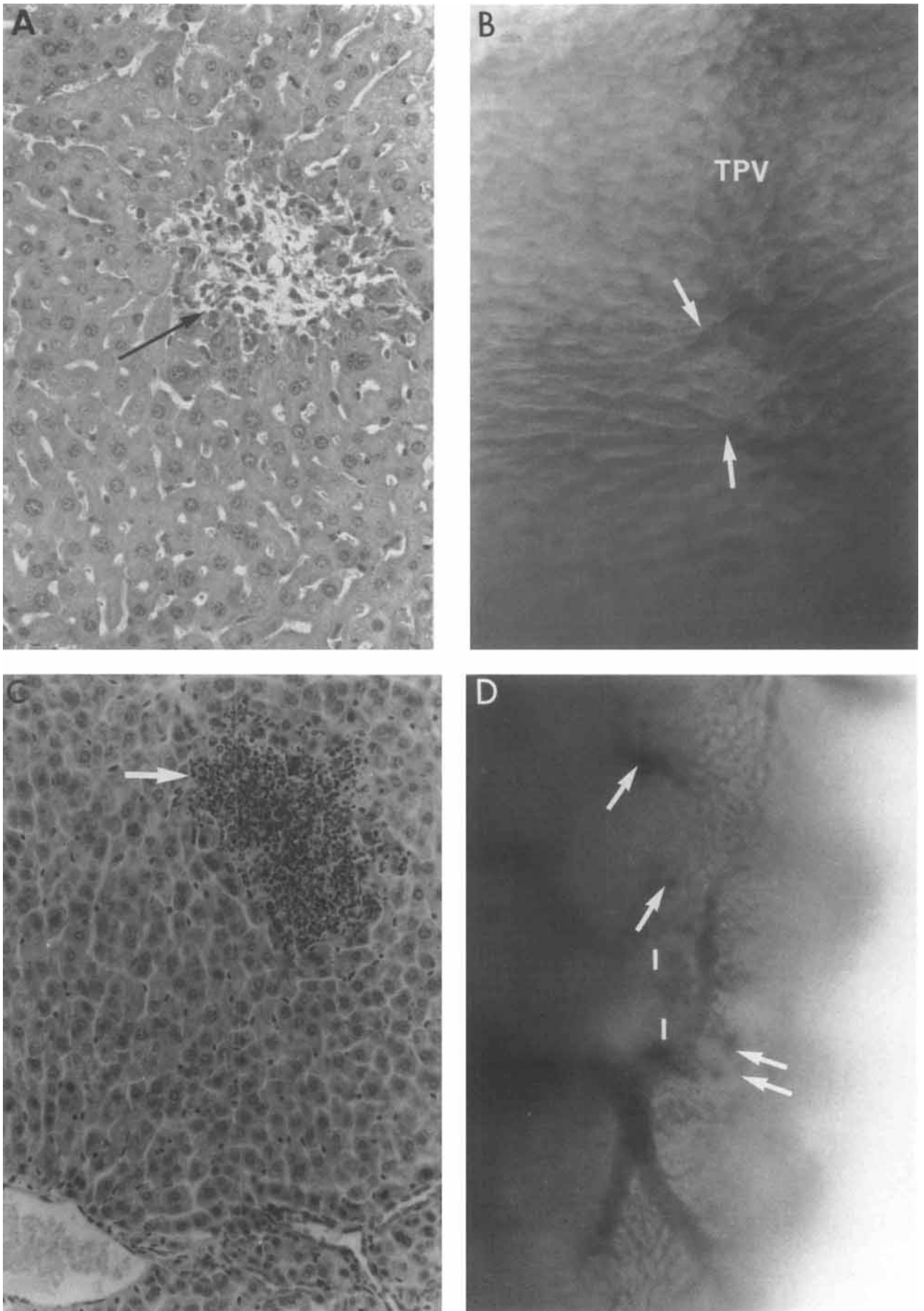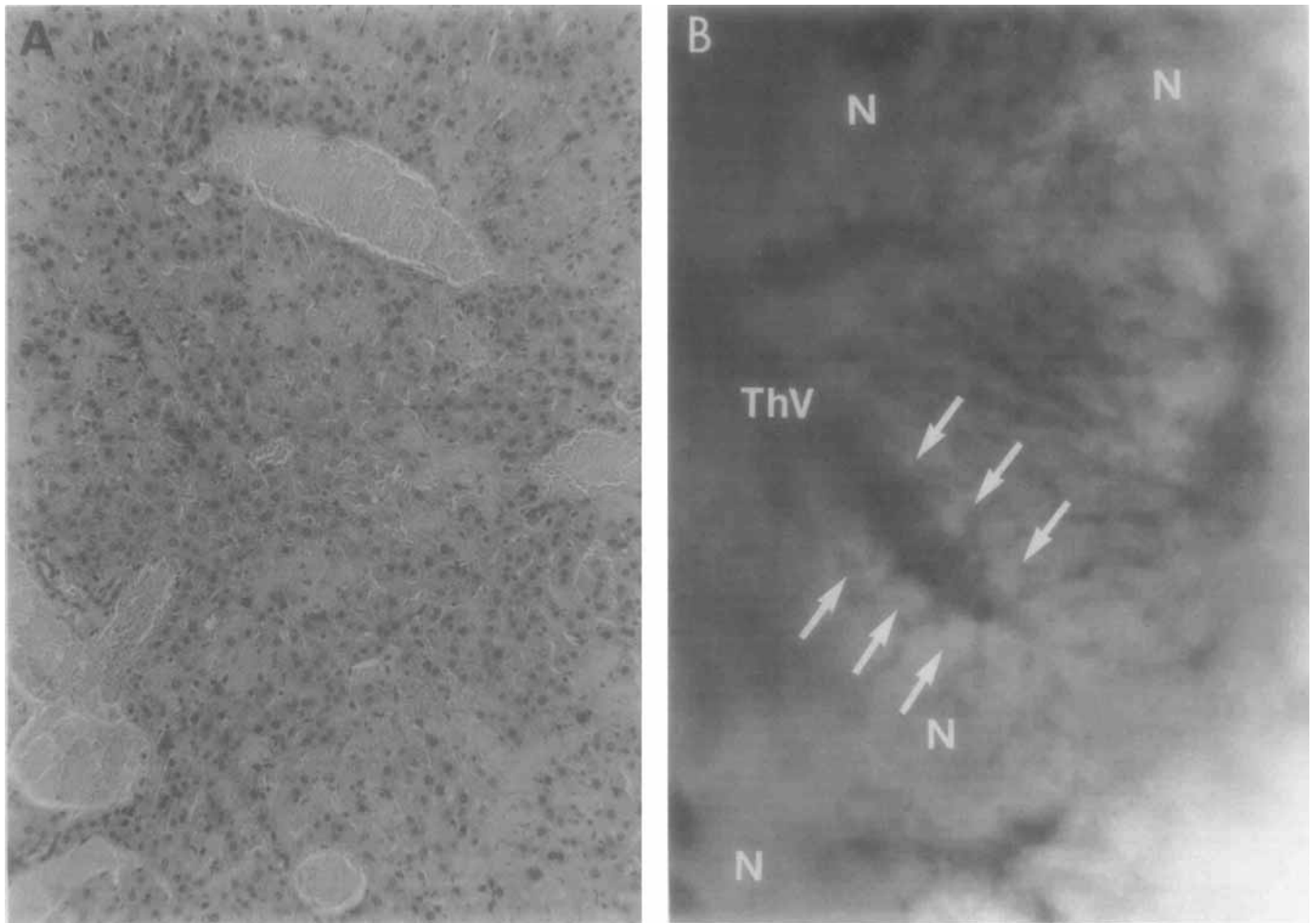
FIG. 2

FIG. 3. Studies of the liver from C3HeB/FeJ mice at 5 days postinfection. (A) Confluent hepatocellular necrosis (H & E, × 350). (B) *In vivo* microscopy of the liver with coalescent necrosis (N), parenchymal edema (*arrow*) adjacent to a terminal hepatic venule (ThV) (× 350).

of disease was observed in approximately 20% of mice. These animals developed an aggressive form of hepatitis characterized by persistent necrotic foci with a mixed inflammatory cell infiltrate, largely mononuclear, a severe terminal portal venule vasculitis and focal hepatocellular dropout (Figure 6A). Both of these groups of animals died within 6 to 9 months of the infection, a marked reduction from the normal 24 to 30 months.

IMMUNOFLUORESCENCE

By indirect immunofluorescence, viral antigens could be detected at 24 hr in both the fully resistant A/J mice and the semiresistant C3HeB/FeJ mice. In the A/J mice, large viral deposits were found within hepatocytes, endothelial cells and Kuppfer cells (Figure 7A). By 48 to 72 hr, antigens were predominantly localized to the cytoplasm of the hepatocytes but some membrane deposition could be seen (Figure 7B). Viral antigens were

detected up to 7 days following infection but were undetectable at Day 10 (Figure 7C).

In livers from C3HeB/FeJ mice, viral antigens were present in the cytoplasm and at the cell surface of hepatocytes at 24 hr postinfection (Figure 8A). By 36 to 48 hr, viral antigens were found in areas of necrosis as well as in apparently normal hepatocytes (Figure 8B). At 7 days, viral antigens were seen in areas of inflammation, which were characterized by a mononuclear cell infiltrate (Figure 8C). For up to 3 months postinfection, viral antigens were detected in both areas of inflammation and morphologically normal hepatocytes (Figure 8D).

VIRAL TITERS

For 12 hr following infection, virus could not be recovered from the livers of either A/J mice or C3HeB/FeJ mice. However, by 24 hr, high titers were detected in both strains of mice (Figure 9). The viral titers peaked

FIG. 2. Studies of livers from C3HeB/FeJ mice following MHV-3 infection. (A) A focal area of necrosis at 24 hr postinfection (*arrow*) (H & E, × 550). (B) *In vivo* microscopy at 24 hr postinfection showing focal blockage of sinusoids (*arrow*) and shunting of blood from the terminal portal venule (TPV) through dilated sinusoids at the margin of the lesion (× 2,250). (C) Large necrotic focus 3 days postinfection which is densely infiltrated with fragmented polymorphonuclear leukocytes (*arrow*) (H & E × 1,125). (D) *In vivo* microscopic studies at 3 days postinfection showing microthrombi (*arrow*) and areas of pale edematous ischemic hepatocytes (I) (× 350).
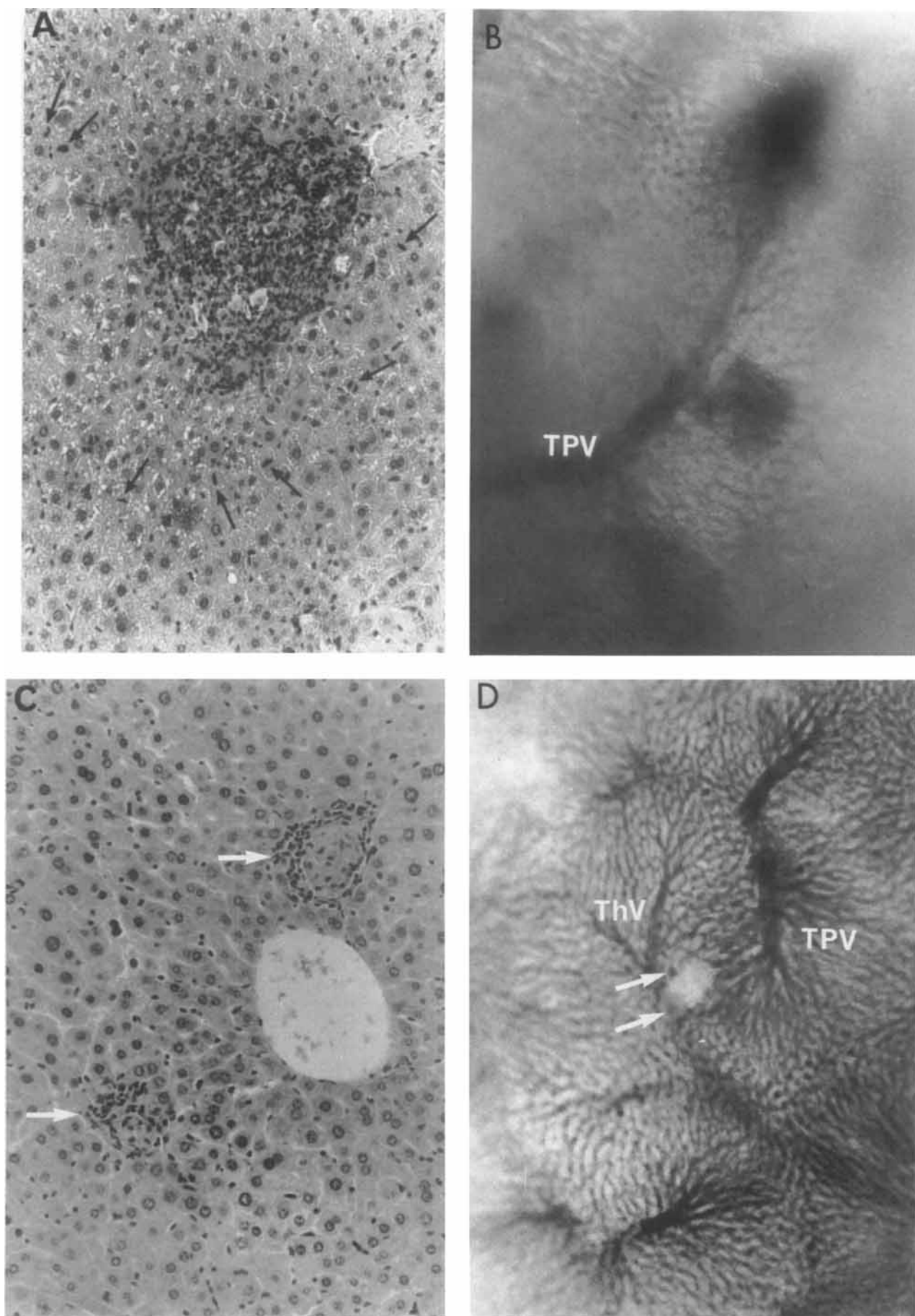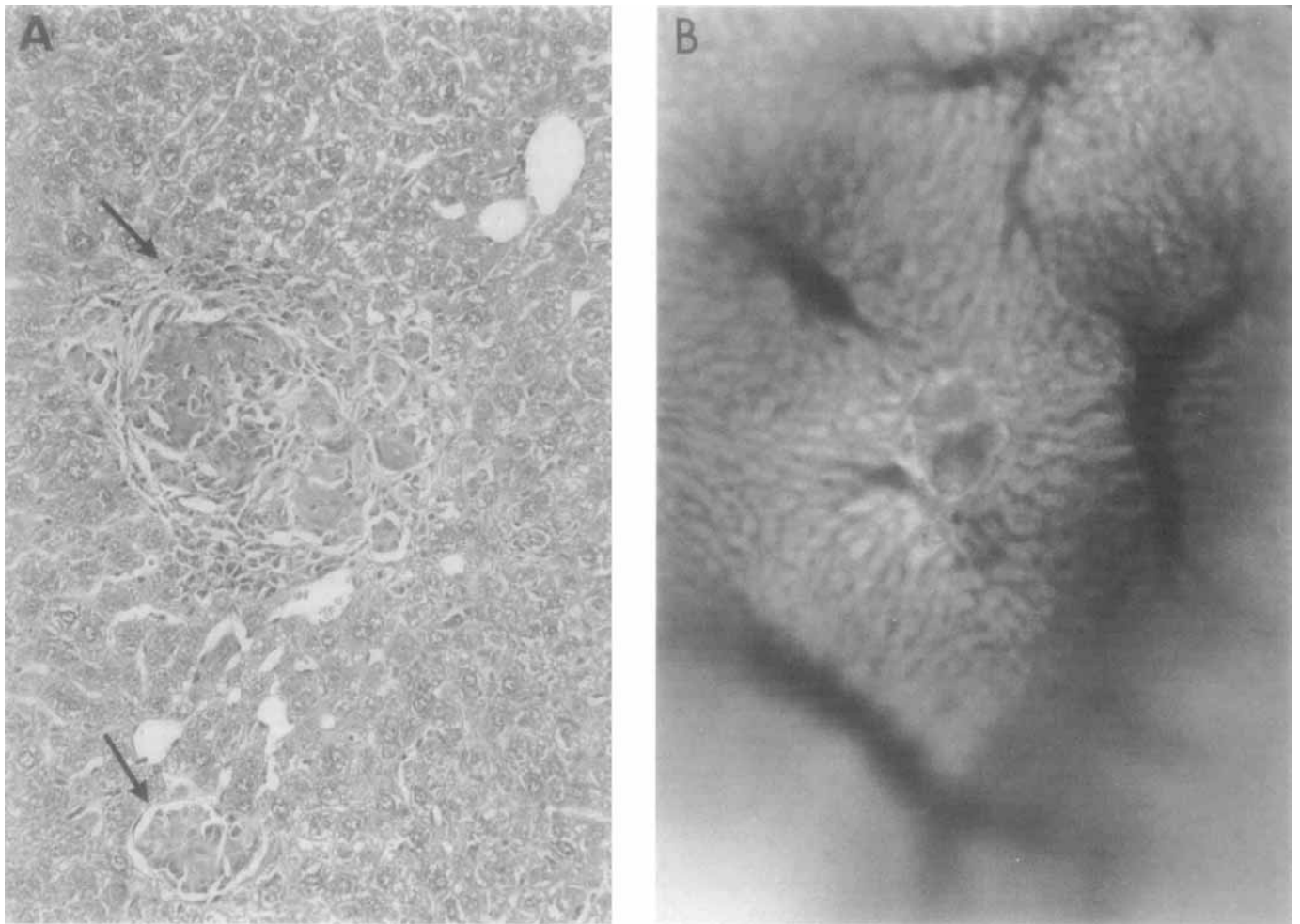
FIG. 4

FIG. 5. Studies of the liver from C3HeB/FeJ mice at 1 month following infection. (A) Giant cell granulomas with a mononuclear cell infiltrate at the periphery (*arrow*). (H & E, × 850). (B) *In vivo* microscopy containing a giant cell granuloma (× 1,125).

by 5 to 7 days postinfection and were no longer detected by Day 7 in A/J mice and by Day 11 in C3HeB/FeJ mice (Figure 9).

PCA

Previously, we have shown that PBM cells, isolated from the blood of uninfected mice and stimulated *in vitro* with MHV-3 responded with an increase in PCA which directly correlated with the *in vivo* susceptibility to hepatic injury in that strain (9).

To determine whether a similar response occurs *in vivo*, PBMs from A/J and C3HeB/FeJ mice were assayed directly following isolation from the blood for both viable (cell surface) and total content PCA (Figure 10). Each PCA determination was made on PBMs from the pooled blood of 10 mice. Mononuclear cells from A/J and C3HeB/FeJ mice which had been injected with 100 μl of DMEM as controls had a basal surface PCA of 20 mU

per 10^6 PBMs. Following infection, there was no increase in PCA in PBMs from fully resistant A/J mice. In C3HeB/FeJ mice, there was a greater than 10-fold increase in viable PCA by 12 hr which reached a maximum 40-fold increase over baseline at Day 4. This elevated PCA persisted for the subsequent 3 to 4 months with minor fluctuations in activity. The values of total PCA (obtained from disrupted cellular homogenates) were approximately twice those expressed at the cell surface (viable), and both activities followed parallel patterns.

In order to examine the PCA response of individual mice, splenic mononuclear cells were harvested from C3HeB/FeJ mice and assayed for total content PCA (Table 1). Early in the course of the infection, all animals had markedly elevated PCA corresponding with the severe histologic and microcirculatory disturbances. At Days 10 to 14, two divergent patterns of PCA were observed. Although in both strains, the PCA remained

FIG. 4. Studies of the liver from C3HeB/FeJ mice following MHV-3 infection. (A) Dense mononuclear cell infiltrate at 7 days postinfection with numerous mitotic figures in hepatocytes (*arrow*) (H & E, × 700). (B) *In vivo* microscopy at 7 days postinfection demonstrating hemorrhagic foci of necrosis adjacent to a terminal portal venule (TPV) (× 550). (C) At 15 days postinfection, epithelioid granulomas scattered throughout the liver parenchyma (*arrow*) (H & E, × 800). (D) *In vivo* microscopy at 15 days postinfection demonstrating a pale well-circumscribed avascular lesion with pigmented cells (*arrow*) at the margin. Terminal portal venule (TPV) and terminal hepatic venule (ThV) are as indicated (× 350).
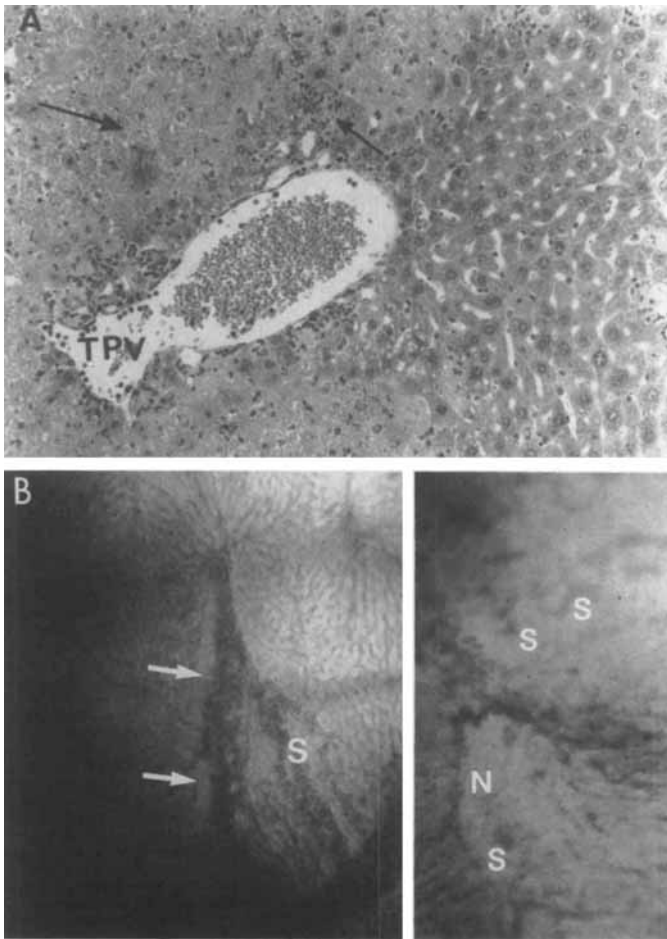
FIG. 6. Studies of the liver from C3HeB/FeJ mice at 1 month postinfection. (A) A focus of aggressive hepatitis with hepatocellular necrosis (*long arrow*), a mixed inflammatory cell infiltrate (*short arrow*) and vasculitis in the terminal portal venule (TPV) (H & E, × 350). (B) *In vivo* microscopy shows clearly in the *inset* severe parenchymal necrosis (N) and sinusoids (S) that are both distorted and distended with stagnant pools of blood with irregular margins of the terminal hepatic vessels (*arrow*) (× 225).

was normal. Small avascular, pale-colored parenchymal lesions, spanning 2 to 3 sinusoids appeared by 24 hr (Figure 2B). Localized granular blood flow, caused by reduced velocity of clumped erythrocytes, was prominent in dilated sinusoids which shunted blood around the lesions. Most of the lesions were found in zone 1 (periportal) of the simple liver acinus with normal intervening parenchyma. At 48 hr, diffuse granular flow occurred in the microcirculation, and sinusoidal microthrombi could be seen (Figure 2D). By 3 to 4 days, the parenchymal lesions were more numerous and larger, spanning as much as a full acinus. Sinusoidal flow was disrupted by microthrombi and edematous hepatocytes, and many sinusoids were dilated with large pools of stagnant blood. At 5 days, parenchymal lesions had coalesced with widespread hepatic necrosis and severe parenchymal edema (Figure 3B). By Days 7 to 10, the diffuse flow abnormality had resolved and many lesions demonstrated dark hemorrhagic centers (Figure 4B). At Day 11, small pale and more sharply circumscribed lesions were noted (Figure 4D). By Day 15, the lesions were further condensed and contained occasional patches of a yellow-green stained pigment. From Day 21 to 2 months, avascular foci of heaped-up tissue were scattered throughout the liver while the intervening parenchyma exhibited normal architecture and sinusoidal blood flow. Histological examination of serial sections showed these lesions to be giant cell granulomas (Figure 5B). In the animals that developed granulomatous hepatitis, *in vivo* microcirculatory flow abnormalities were confined to the sinusoids surrounding the granulomatous lesions. This consisted largely of granular blood flow at the periphery of the granuloma, and no blood flow was observed through the granuloma itself. Histologic examination demonstrated large numbers of mononuclear cells in the sinusoids adjacent to the lesions. In approximately 20% of C3H/eBFeJ mice, marked localized abnormalities of the liver microcirculation correlated histologically with foci of aggressive hepatitis (Figure 6B). These foci were composed of a central avascular core which was surrounded by pale edematous hepatocytes containing dilated and disorganized sinusoids with slow or absent blood flow. Subsequent histologic analysis of these lesions which had been studied *in vivo* demonstrated large areas of necrosis with a marked predominantly mononuclear inflammatory cell infiltrate (Figure 6A).

elevated, animals that developed severe hepatitis (Type 1) maintained the high levels of PCA found during the acute phase of the disease whereas animals that developed chronic granulomatous hepatitis (Type 2) had PCA elevations at 5 to 10 times background but only 25 to 30% of the PCA observed in Type 1 animals. No increase in total PCA was found in PBMs or splenic macrophages from A/J mice over initial basal values.

HEPATIC MICROCIRCULATION

In vivo microscopy of normal control A/J and C3HeB/FeJ mice that had received 100 µl i.p. of DMEM revealed normal streamlined blood flow of the terminal hepatic vessels and the sinusoids (Figure 1B). Blood flowed from the terminal portal venules, with occasional bursts of arteriolar flow, into the proximal sinusoids. The blood could be followed as it drained into terminal hepatic venules. Liver cell cords 1 to 2 cells wide separated the sinusoids. At 12 hr postinfection in C3HeB/FeJ mice, the velocity of blood flow in the terminal hepatic vessels was slowed, however, the architecture of the parenchyma

DISCUSSION

The outcome of viral infection in a host is the result of a complex set of interactions between the elements of the immune system, host cells and the virus (13, 14). A number of immune effector networks have been studied in the model of murine hepatitis virus infection; however, to date, none of these have shown good correlation with the strain dependence of disease susceptibility (15, 16). In this paper, we present data that associate the spontaneous expression of monocyte PCA with acute and chronic liver inflammation in MHV-3-induced hepatitis. This relationship emphasizes the possible role of the coagulation cascade in the disturbances of the microcirculation that enhance liver cell necrosis.
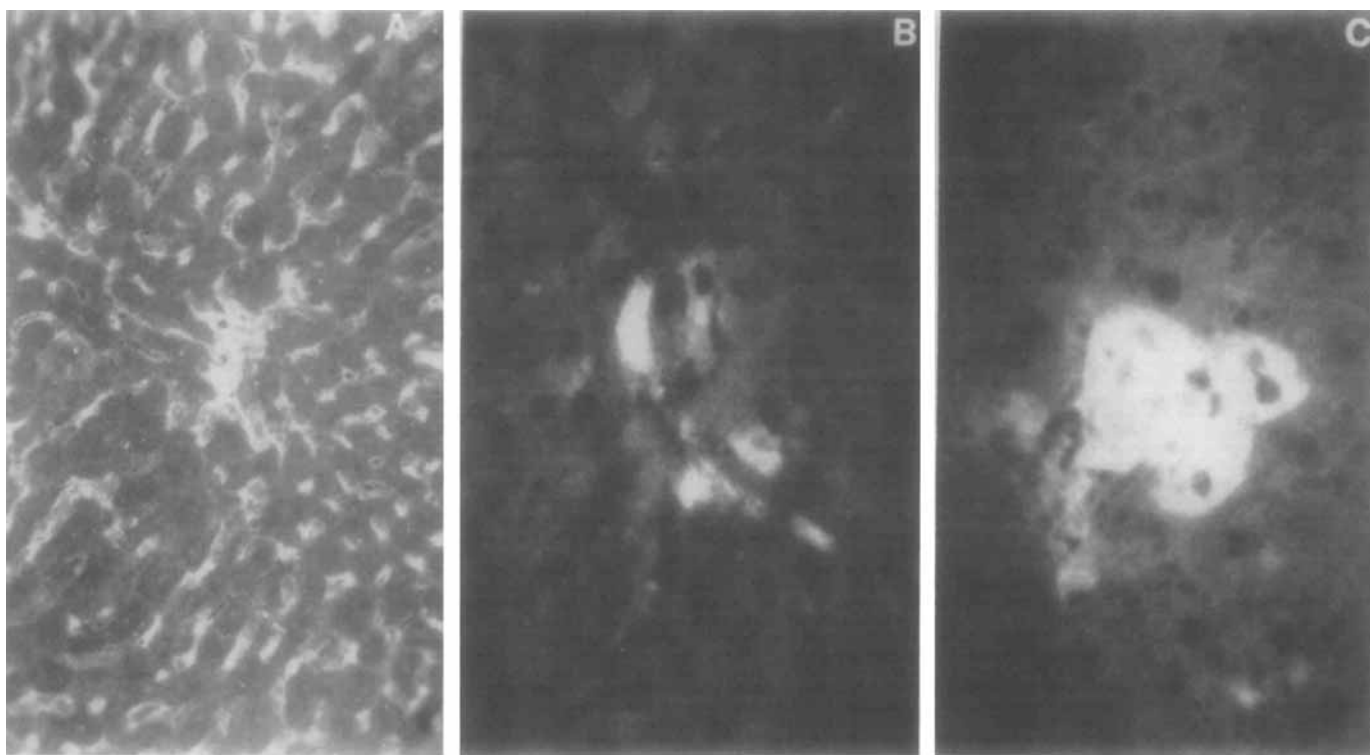
FIG. 7. Indirect immunofluorescence studies of livers from MHV-3-infected A/J mice. (A) At 24 hr postinfection, antigens can be seen distributed diffusely throughout the liver, localized mainly in sinusoidal lining cells with occasional deposits in the cytoplasm of hepatocytes (× 500). (B) At 48 hr, viral antigens are predominantly localized to the cytoplasm of hepatocytes (× 500). (C) At 7 days, virus can be detected in hepatocytes both in the cytoplasm and at the cell surface (× 500).

Activation of the coagulation system is a common feature of inflammation (17–20). Activated coagulation proteins serve as mediators of the inflammatory response by in turn recruiting the complement, kallikrein-kinin and fibrinolytic systems (20). Furthermore thrombin and its activation fragment 1.2 directly elicit chemotaxis in monocytes (21). It has been known for several years that leukocytes express a number of PCAs following stimulation both in vitro and in vivo (20, 22). The cellular source of this activity is the monocyte/macrophage but T lymphocytes and/or their products are necessary for the induction of these procoagulant monokines (22). The coagulation cascade may be activated at local sites of inflammation by the procoagulant products of infiltrating leukocytes resulting in amplification of the inflammatory response with increased tissue injury.

The pattern of spontaneous monocyte PCA observed in these experiments in the A/J and C3HeB/FeJ mice is in agreement with the previously described direct correlation of monocyte PCA with susceptibility to liver disease following MHV-3 infection of PBM with MHV-3 in vitro (8, 9). In the C3HeB/FeJ mice, a constant proportion (50%) of PCA was expressed at the cell surface, consistent with the physiologic importance of PCA in situ. During the early stage of the infection, splenic macrophage PCA did not discriminate between those mice that develop chronic aggressive hepatitis or chronic granulomatous hepatitis. Only by Day 10 could distinct patterns of PCA response be identified, and these correlated with the severity of the histologic lesion (Table

1). As the mice studied are inbred strains, it is apparent that factors other than genetic are involved in the evolution of the immune-inflammatory process. Other investigators have shown that diet, age, sex, stress and temperature affect immune responses to infectious processes (23). However, in studies using recombinant inbred strains of mice, we have shown that PCA and susceptibility/resistance to MHV-3 infection are genetically linked and are controlled by two independent non-H-2-linked genetic loci (Dindzans, V. et al., Hepatology 1984; 4:1053, Abstract). Determinations of β-glucuronidase, 5'-nucleotidase and elastase in macrophages from MHV-3 infected and control animals did not correlate with susceptibility to infection and resultant hepatitis (24) and thus, monocyte PCA is not simply a nonspecific marker of inflammation.

The immunofluorescence studies and viral titers in the resistant A/J mice demonstrate that permissiveness to viral replication alone cannot explain the disease observed. In addition, the abnormalities in the microcirculation following MHV-3 infection were detected prior to viral replication. Evidence for a role of the microcirculation in the pathogenesis of acute hepatitis has been generated by in vivo microscopic studies of the liver during toxic hepatitis. Severe flow abnormalities, consisting of sinusoidal constriction and dilation, granular blood flow, microhemorrhages and microthrombi, are prominent features of toxic hepatitis (25). During hepatitis caused by toxic agents, microcirculatory abnormalities begin in a zonal distribution with the most severe
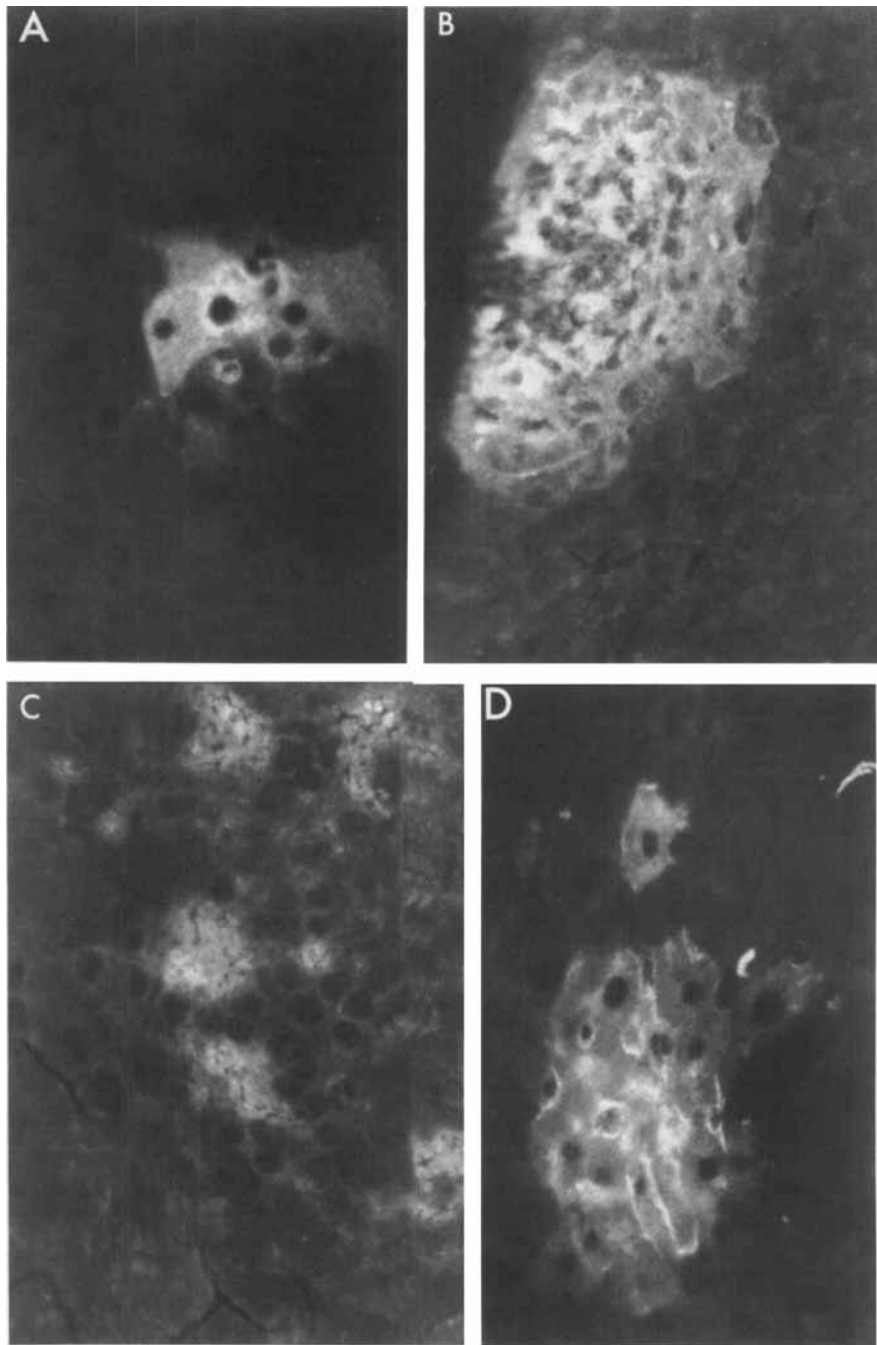
FIG. 8. Indirect immunofluorescence studies of livers from MHV-3-infected C3HeB/FeJ mice. (A) At 24 hours viral antigens are found in small foci of hepatocytes ($\times$ 500). (B) At 48 hours viral antigens are found localized both in areas of necrosis as well as in viable hepatocytes ($\times$ 500). (C) At 7 days postinfection viral antigens are found in both foci of necrosis as well as in viable hepatocytes ($\times$ 500). (D) At 1 month postinfection, viral antigens are still detectable in hepatocytes both in the cytoplasm and at the cell surface ($\times$ 500).

changes occurring in areas of greatest hepatocellular damage (5, 6, 26).

The earliest abnormality seen following MHV-3 infection *in vivo* was granular blood flow, a relatively nonspecific finding whose mechanism has been attributed to several factors (27, 28). These include: hypotension, neurally mediated vasoconstriction and vasodilation, humoral mediators (histamine, bradykinin) of vasodilation, hemoconcentration due to capillary permeability increases and changes in the surface charge of erythrocytes due to fibrin adsorption. Studies using fluorescent-labeled proteins during the acute phase of allyl formate hepatitis revealed increased sinusoidal permeability within 10 min of administration of the toxin, coincident with the appearance of granular flow (6). Similar abnormalities were detected in MHV-3-infected C3HeB/FeJ mice, suggesting similar pathophysiological mechanisms may be operative.
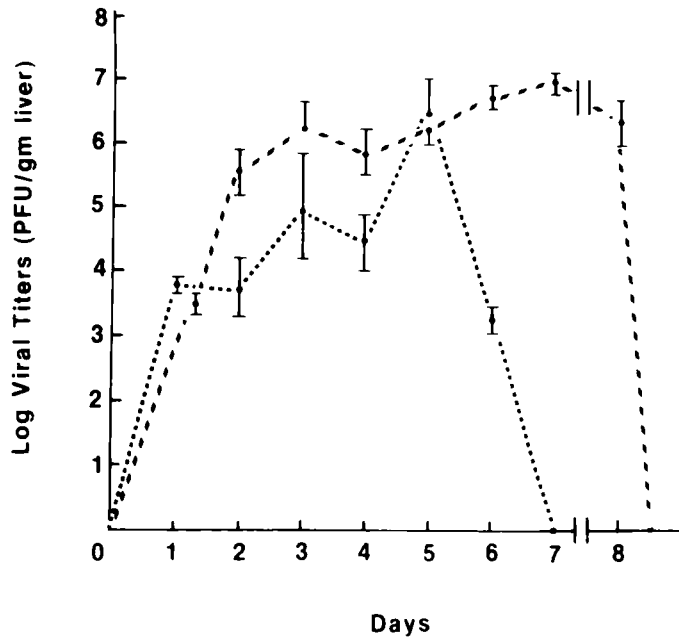
FIG. 9. Recovery and growth of MHV-3 from the livers of A/J and C3HeB/FeJ mice. MHV-3 was recovered in high titers from both A/J mice (- - - -) and C3HeB/FeJ mice (▬) throughout the course of the infection.
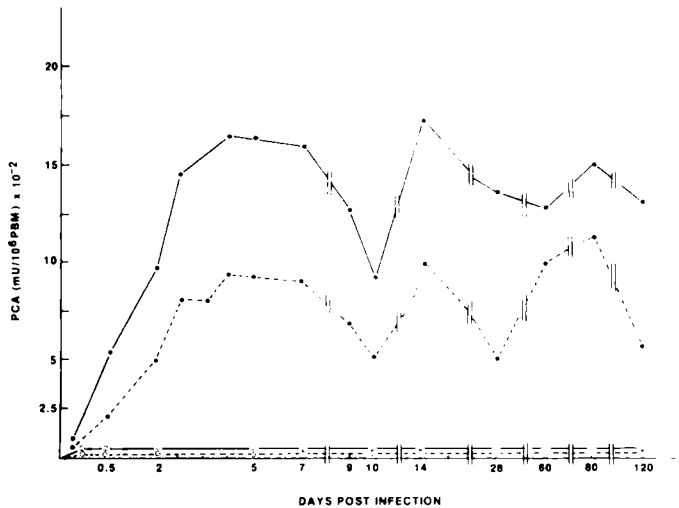

FIG. 10. Spontaneous expression of monocyte PCA in A/J and C3HeB/FeJ mice. A marked rise in both viable (●- - - -●) as well as total content monocyte PCA (●———●) could be found in monocytes isolated and analyzed from C3HeB/FeJ mice, whereas no detectable PCA response either viable (O   -O) or total content (O———O) in monocytes from A/J mice was observed.

We postulate that the earliest derangement in hepatic physiology during MHV-3 infection is consequent to the viral-induced generation of monocyte/macrophage PCA resulting in activation of the coagulation cascade. This, in turn, could trigger the complement and kallikrein systems resulting in bradykinin-mediated vasodilation, increased vascular permeability and eventually granular blood flow. Under the influence of potent chemotactic factors (C3a, C5a, C567 and thrombin), circulating leukocytes would be recruited to the areas of inflammation. Continued elaboration of PCA by monocytes and possibly Kupffer cells would further amplify the original re-

TABLE 1. SPLENIC MACROPHAGE PCA IN MHV-3 INFECTED C3HeB/FeJ MICE

Days postinfection[a]	PCA[b] (mU/10⁶ splenic macrophages)	
	Type 1[c]	Type 2[d]
−1	125 ± 10	145 ± 15
0.5	2,450 ± 150	2,750 ± 245
3	5,850 ± 400	4,650 ± 500
7	4,400 ± 175	3,950 ± 250
10	4,850 ± 200	2,150 ± 175
14	3,975 ± 375	1,845 ± 210
21	4,475 ± 550	1,475 ± 100
60	3,950 ± 210	975 ± 50
90	4,875 ± 350	1,200 ± 75

[a] Mice were infected with 1,000 plaque-forming units of MHV-3 i.p.

[b] Spontaneous PCA determined on splenic macrophages in a one-stage clotting assay and represents the mean ± S.D. on five animals at each time point.

[c] Type 1 refers to C3HeB/FeJ mice that go on to develop chronic aggressive hepatitis.

[d] Type 2 refers to C3H/eB/FeJ mice that develop chronic granulomatous hepatitis.

sponse. During the acute phase, sinusoidal blockage by microthrombi, in concert with simultaneous viral replication within sinusoidal lining cells and hepatocytes (with disruption of mitochondria and endoplasmic reticulum), may render the hepatocytes were susceptible to ischemic damage and injury by inflammatory mediators (29). Hepatocellular necrosis, leukocyte infiltration and edema may result in further sinusoidal blockage and potentiation of the parenchymal damage. Such microcirculatory abnormalities have been observed in vivo following the administration of lipopolysaccharide, a potent activator of both the coagulation cascade and monocyte PCA (12, 30, 31).

In the acute phase of MHV-3 infection, viral antigens were diffusely deposited in the liver, and extensive microcirculatory disturbances were observed. In contrast, during the chronic phase, viral antigens were localized in focal deposits. Thus, continued specific stimulation of PCA in the chronic phase may result in localized microcirculatory disturbances confined to the areas of antigen deposition. Since it is known that PCA directly correlates with in vitro and in vivo measures of delayed cutaneous hypersensitivity (23), it is conceivable that PCA exerts its influence through both cellular and humoral immune mechanisms. This could occur by the production of lymphokines and/or the recruitment of activated T cells macrophages and NK cells into the chronically affected area. Finally, since PCA is a potent serine protease, it may have effects through its proteolytic action on substrates other than prothrombin.

As an example, one of the earliest pathologic features of experimental allergic hepatitis is the deposition of immune complexes within the sinusoids (32). This is followed by thrombotic occlusion of sinusoids with resultant focal coagulative necrosis (32). A similar pathologic mechanism has been proposed for fulminant hepatitis B (33). We have previously reported that immune complexes stimulate the production of PCA, thus asso-

ciating the production of immune coagulants with liver injury (24, 34).

In this paper, we present further evidence suggesting a link between viral induction of monocyte/macrophage PCA and disturbances in the microcirculation in liver disease.

REFERENCES

1. Greenway CV, Stark RD. Hepatic vascular bed. Physiol Rev 1971; 51:23–65.
2. Rappaport AM. The microcirculatory acinar concept of normal and pathological hepatic structure. Beitr Pathol Bd 1976; 157:215–243.
3. Gumucio JJ, Miller DL. Functional implications of liver cell heterogeneity. Gastroenterology 1981; 80:393–403.
4. Chen FH, Gumucio JJ, Ho NH, et al. Hepatocytes of zones 1 and 3 conjugated sulfobromopthalein with glutathione. Gastroenterology 1984; 4:467–476.
5. Nakata K, Fujimoto K. Relationship between liver cell injury and circulatory disturbances in the development of CCl4 toxicity. Acta Pathol Japan 1973; 23:667–673.
6. Chernukh AM, Kwalenko NY. Disorders of microcirculation and vascular tissue permeability in acute diffuse experimental hepatitis. Bibl Anat 1973; 12:484–489.
7. Wege H, Sidell S, ter Meulen V. The biology and pathogenesis of coronaviruses. Curr Top Microbiol Immun 1982; 99:131–163.
8. Levy GA, MacPhee PJ, Fung LS, et al. The effect of mouse hepatitis virus infection on the microcirculation of the liver. Hepatology 1983; 3:964–973.
9. Levy GA, Leibowitz JL, Edgington TS. Induction of monocyte procoagulant activity by murine hepatitis virus type 3 parallels disease susceptibility in mice. J Exp Med 1981; 154:1150–1163.
10. Le Provost C, Virelizier JL, Dupuy JM. Immunopathology of MHV-3 infection. III. Clinical and virologic observations of a persistent viral infection. 1975; 115:640–643.
11. Leibowitz JL, Fung LS, Levy GA. A sensitive radioimmunoassay for the detection of antibody to mouse hepatitis. J Virol Methods 1983; 3:255–265.
12. Levy GA, Edgington TS. Lymphocyte cooperation is required for amplification of macrophage procoagulant activity. J Exp Med 1980; 151:1232–1244.
13. Mims CA. Aspects of the pathogenesis of virus diseases. Bacteriol Rev 1964; 28:30–71.
14. Buchmeier MJ, Welch RM, Dutko FJ, et al. The virology and immunobiology of lymphocytic choriomeningitis infection. Adv Immunol 1980; 30:275–331.
15. Schindler L, Engler H, Kirchner H. Activation of natural killer cells and induction of interferon after injection of mouse hepatitis virus type 3 in mice. Infect Immunol 1982; 35:869–873.
16. MacNaughton MR, Patterson S. Mouse hepatitis virus-3 infection of C57, A/Sn and A/J strain mice and their macrophages. Arch Virol 1980; 66:71–75.

17. Zimmerman TS, Freier J, Rothberger H. Blood coagulation and the inflammatory response. Semin Hematol 1977; 14:391–408.
18. Levy GA, Helin H, Edgington TS. The pathobiology of viral hepatitis and immunologic activation of the coagulation protease network. Semin Liver Dis 1984; 4:59–68.
19. Thompson NM, Simpson IS, Peters DK. A quantitative evaluation of anti-coagulants in experimental nephrotic nephritis. Clin Exp Immunol 1975; 19:301–312.
20. Sundsmo JS, Fair DS. Relationships among the complement, kinin, coagulation and fibrinolytic systems in the inflammatory reaction. Clin Physiol Biochem 1983; 1:225–284.
21. Bar-Shevit R, Kahn A, Wilner GD. Monocyte Chemotaxis: stimulation by specific exosite region in thrombin. Science 1983; 220:728–731.
22. Edgington TS, Helin H, Gregory SA, et al. Cellular pathways and signals for the induction, biosynthesis of initiators of the coagulation protease cascade and of plasminogen activators in cells of the monocyte lineage. Monocytes, macrophages and inflammation. Amsterdam: Elsevier North-Holland, 1984 (in press).
23. Geczy CL. The role of lymphokines in delayed type hypersensitivity reactions. Springer Semin Immunopathol 1984; 7:321–346.
24. Dindzans VJ, MacPhee PJ, Fung LS, et al. The immune response to mouse hepatitis virus: expression of monocyte procoagulant activity and plasminogen activator during infection in vivo. J Immunol (in press).
25. Rappaport AM. Physioanatomical basis of toxic liver injury. In: Farber E, Fisher MM, eds. Toxic injury of the liver. New York: Marcel Dekker Publishers, 1973: 1–57.
26. Rappaport AM, MacDonald A. Study of the effects of acetaminophen (paracetamol) on the hepatic microcirculation. In: Grayson J, Zingg W, eds. Microcirculation: first world congress on microcirculation. University of Toronto 1975, Vol 1. New York: Plenum Press, 1975: page 350.
27. Nagler A. The circulatory manifestations of bacterial endotoxemia. In: Kaley G, Altura BM, eds. Microcirculation, Vol 3. Baltimore, Maryland: University Park Press, 1980: 107–117.
28. Bloch EH. Microscopic observations of the circulating blood in the bulbar conjunctiva in man in health and disease. Ergebenisse der Anatomie und Entwicklungs Geshichte 1956; 35:1–98.
29. Reubner BH, Hirano T, Slusser RJ. Electron microscopy of the hepatocellular and Kupffer cell lesion of mouse hepatitis with particular reference to the effect of cortisone. Am J Pathol 1967; 51:163–189.
30. McCluskey RS, Urbaschek R, McCluskey PA, et al. In vivo studies of the responses of the liver to endotoxin. Klin Wochenschr 1982; 60:749–751.
31. Goodman ML, Way BA, Irwin JW. The inflammatory response to endotoxin. J Pathol 1979; 128:7–14.
32. Sabesin SM. Electron microscopy of hypersensitivity reactions: allergic hepatic necrosis. Am J Pathol 1963; 42:743–754.
33. Mondelli M, Eddleston ALWF. Mechanisms of liver cell injury in acute and chronic hepatitis B. Semin Liver Dis 1984; 4:47–58.
34. Schwartz BS, Levy GA, Edgington TS. Immune complex induced human monocyte procoagulant activity. II. Cellular kinetics and metabolic requirements. J Immunol 1982; 128:1037–44.